Palaeogeography, Palaeoclimatology, Palaeoecology 306 (2011) 75–81

Contents lists available at ScienceDirect

Palaeogeography, Palaeoclimatology, Palaeoecology

journal homepage: www.elsevier.com/locate/palaeo

Interannual climate variability in the Miocene: High resolution trace element and stable isotope ratios in giant clams

Sietske J. Batenburg [a,*], Gert-Jan Reichart [a,b], Tom Jilbert [a], Max Janse [c], Frank P. Wesselingh [d], Willem Renema [d]

[a] Utrecht University, P.O. box 80021, 3508 TA Utrecht, The Netherlands
[b] Alfred Wegener Institute for Polar and Marine Research, Am Handelshafen 12, 27570 Bremerhaven, Germany
[c] Burgers' Zoo, Antoon van Hooffplein 1, 6816 SH Arnhem, The Netherlands
[d] Nederlands Centrum voor Biodiversiteit Naturalis, Darwinweg 2, 2333 CR Leiden, The Netherlands

ARTICLE INFO

Article history:
Received 15 June 2010
Received in revised form 24 February 2011
Accepted 30 March 2011
Available online 8 April 2011

Keywords:
Tridacna
Oxygen isotopes
Carbon isotopes
Mg/Ca
ENSO
Miocene

ABSTRACT

High resolution stable isotope and trace elemental ratios of a recent *Tridacna squamosa* from Vietnam and a Middle to Late Miocene (10–13 Ma) *Tridacna gigas* from Indonesia are presented. The seasonal pattern of modern sea surface temperature (SST) variability offshore Vietnam is faithfully recorded in the $\delta^{18}O$ of the *T. squamosa* shell carbonate, confirming the potential of *Tridacna* shells as sub-annual resolution climate archives. Cultivation of the *T. squamosa* specimen in controlled conditions after recovery from the natural environment facilitated a quantitative calibration of the $\delta^{18}O$ signal to ambient water temperatures. An age model for the Miocene *T. gigas* shell from Indonesia was therefore constructed on the basis of its $\delta^{18}O$ profile, assuming a single-peak annual SST cycle. The magnitude of these oscillations was 5–7 °C. Mg/Ca and the growth-banding pattern in the Miocene *T. gigas* correlates well with shell $\delta^{18}O$ during the later part of the organism's lifespan. Ba/Ca is negatively correlated to Mg/Ca, with a lag of several months, suggesting a different phasing of the annual primary productivity cycle from that of SST. Furthermore, $\delta^{18}O$ and Mg/Ca show prominent deviations to warmer conditions with a periodicity of ~3 years. These shifts demonstrate the existence of substantial interannual sea surface temperature variability in the Miocene, a period with elevated global temperatures compared to the present day.

1. Introduction

Interannual climate variability in the modern Pacific Ocean is dominated by the El Niño Southern Oscillation (ENSO). Sea surface temperatures (SST's) in the western equatorial Pacific Ocean are generally higher, and the thermocline is deeper compared to the eastern equatorial Pacific, due to the piling-up of warm water in the west. Every few years the east-west gradient collapses into El Niño-like conditions as the so-called Pacific Warm Pool moves eastward. This results in drought in the western, and increased precipitation and reduced upwelling in the eastern Pacific (Cane, 2005; Wang and Fiedler, 2006). During El Niño events, cold SSTs and a shallow thermocline are observed along the Indian Ocean coasts of Java, Timor and Sumatra (Meyers, 1996; Kuhnt et al., 2004). When the system returns to its normal state, it sometimes "overshoots", resulting in a 'La Niña', a state of extreme east–west contrast.

The stability of ENSO in a future warmer climate is uncertain (Cane, 2005). Hence, recent research has focused on reconstructing the occurrence of ENSO-type climate variability during past warmer climates. Increased global temperatures have been suggested to trigger a permanent El Niño-like state, due to a globally-deeper thermocline (Fedorov et al., 2006). Several studies have focused on the warm Early Pliocene (5–3 Ma), reconstructing SST gradients and thermocline depth differences across the tropical Pacific Ocean (Chaisson, 1995; Rickaby and Halloran, 2005; Wara et al., 2005; Ravelo et al., 2006). Foraminiferal assemblages (Chaisson, 1995) and $\delta^{18}O$ records from planktonic foraminifera (Ravelo et al., 2006) suggest that the east–west gradient in surface water conditions was reduced during the warm Early Pliocene compared to today, similar to present day El Niño-like conditions. Mg/Ca ratios measured in planktonic foraminiferal shells suggest that the eastern equatorial Pacific was ~2.5 °C warmer and the western equatorial Pacific ~2 °C cooler than today (Wara et al., 2005). Furthermore, SST reconstructions based on the alkenone unsaturation index ($U^{k'}_{37}$) indicate that the eastern equatorial Pacific was ~2.5 °C warmer during the Early Pliocene than today (Ravelo et al., 2006). Overall, these results support the hypothesis that during the warm Early Pliocene, east–west asymmetry in SST and thermocline depth was reduced compared to present day, implying 'permanent' El Niño-like

* Corresponding author at: Present address: Istituto per l'Ambiente Marino Costiero (IAMC-CNR) Calata Porta di Massa, Porto di Napoli, 80133 Napoli, Italy. Tel.: +39 3409952309, +39 0815423859; fax: +39 815423888.
E-mail address: sbatenburg@gmail.com (S.J. Batenburg).

0031-0182/$ – see front matter © 2011 Elsevier B.V. All rights reserved.
doi:10.1016/j.palaeo.2011.03.031

conditions (Ravelo et al., 2006). However, due to limitations of sampling resolution, such sediment-based reconstructions cannot provide direct information about the presence of inter-annual climate variability. Annually resolved archives are a prerequisite for the direct assessment of seasonal to inter-annual climate variability in the Pacific region.

Here we present stable isotope and trace elemental records from two giant clam shells. Giant clams are the largest living bivalve mollusks, with growth rates of on average 1 cm per year (Bonham, 1965), and can live up to several decades. They have a broad geological distribution and occur in the fossil record since the Eocene (Watanabe et al., 2004). Giant clams have some advantages over corals for the retention of seasonal-scale proxy records. Corals can suffer from kinetic effects on isotope fractionation during carbonate precipitation (McConnaughey, 1989; Aharon, 1991) and easily undergo diagenetic overprinting (McGregor and Gagan, 2003), whereas giant clams precipitate carbonate near isotopic equilibrium with seawater (Aharon, 1991) and have very dense aragonitic shells. We present records of a recent *Tridacna squamosa* (Lamarck, 1819) from Vietnam and a Miocene *Tridacna gigas* (Linnaeus, 1758) from Indonesia. Tridacnid clams have daily growth increments (Aharon and Chappell, 1986; Watanabe et al., 2004), allowing very high resolution sampling and providing excellent age control. We use these records to demonstrate the sensitivity of *Tridacna* shell chemistry to interannual environmental variability, and to reconstruct such variability during a short window of the Miocene.

2. Materials and methods

A well-preserved *Tridacna gigas* shell was taken from the K. Martin collection (catalogue number RGM 5444) in the Nederlands Centrum voor Biodiversiteit Naturalis in Leiden, the Netherlands. The specimen was collected in 1910 by K. Martin and his wife H. Martin-Icke in the area west of Bandung on the island Java, Indonesia (Fig. 1). Since all the fossil beds were considered to be of the same formation, the Nyalindung beds, and because of the habit to label fossils by general locality (often village or river names), some uncertainty about the exact locality and age of the fossils exists. In 1911, immediately after their return to the Netherlands, Martin published a preliminary description of the localities, listing all the gastropods (Martin, 1911). The age of the locality Tji Angsana was indicated as 'Jung Miocän', which included the current Middle and Late Miocene. In 1919 he described the area in detail (Martin, 1919), and it turned out that there are a series of localities in the riverbed of Tji Angsana. The locality described in 1911 was the stratigraphically lower one, and a series of localities (five in total) were found overlying these beds near the village of Kampung Angsana. All corals and *Tridacna* from Tji Angsana were collected from these overlying beds (Gerth, 1921). The river bed section has a very similar fauna to the nearby Tji Talahab locality, for both mollusks and foraminifera (Martin, 1921; van der Vlerk, 1921). In these localities the biostratigraphically important large benthic foraminifera *Nephrolepidina (Trybliolepidina) rutteni*, miogypsinids (van der Vlerk, 1921) and *Alveolinella fennemai* (pers. obs WR in Naturalis collection) have been found, indicating Tf2 (=~Langhian, 16–14 Ma). Additionally, in Tji Angsana a well preserved foraminiferal fauna is found containing *Amphisorus martini* (identified as *Marginopora vertrebralis*), *Alveolinella quoyi* (identified as *Alveolinella* sp. and the descendant of *A. fennemai*) and some smaller benthic foraminifera (van der Vlerk, 1921). Next to the above mentioned species, sediments in the Naturalis collection contained very rare *N. (Trybliolepidina) rutteni* with a larger deuteroconch and more adauxilary chambers than those from Tji Talahab and the riverbed (pers. obs. WR). These all indicate a younger age for the Tji Angsana locality where the *Tridacna* has been found, most likely referable to the last part of the Serravallian and base of the Tortonian, ~10–13 Ma.

A calibration of $\delta^{18}O$ versus temperature was performed with a recent *Tridacna squamosa* specimen, which has grown under controlled conditions for several years. This specimen was captured alive in Vietnam and placed in an aquarium with a coral reef setting in Burgers' Zoo, Arnhem, the Netherlands. Whereas seasonal variations in temperature off the coast of Vietnam are pronounced (maximally 5 °C, Xie et al., 2003), seasonal variability in the aquarium was low, with little daylight penetrating the aquarium and very stable temperature conditions (25.9 °C with a standard deviation of only 0.19 °C).

Of both shells, a slice of approximately 0.5 cm thick was cut perpendicular to the growth direction, polished and cleaned with ethanol to reveal growth increments. In the recent *Tridacna squamosa* shell, individual daily growth increments could be observed. A distinct transitional surface separates the part of the shell grown in Vietnam and the part grown in Burgers' Zoo. In the Miocene *Tridacna gigas* specimen, small scale lineation is present, but individual growth increments could not be distinguished. However, the specimen had approximately 11 darker bands which, in giant clams, are annual in nature (Bonham, 1965; Aharon, 1991).

Samples of carbonate powder for stable isotope analysis were obtained with a computer operated micromill device (Mercantek). Grooves of approximately 4 to 6 mm long and 100 μm in width were drilled parallel to growth line direction and at least 300 μg of material was collected from each sample. In the *Tridacna squamosa* shell, samples were taken approximately every ten growth increments, of which the distance was measured to assess growth rates. In the *Tridacna gigas*, samples were taken every 0.5 mm.

From each sample 30 to 50 μg was analyzed for stable isotopes on an automated carbonate preparation device (CARBO-KIELIII), linked on-line to a mass spectrometer (MAT Finnigan 253). The international standard NBS-19 and the in-house standard Naxos were used for calibration, and the analytical one-sigma precision was better than 0.05‰ for $\delta^{13}C$ and better than 0.08‰ for $\delta^{18}O$.

Trace elemental composition was determined by LA-ICP-MS (Laser Ablation-Inductively Coupled Plasma-Mass Spectrometer), with a Geolass200Q Excimer 193 nm laser coupled to a Micromass Platform ICP-MS. NIST SRM 610 was used for calibration with ^{44}Ca as internal standard. A fluence of 4 J cm^{-2} was applied. Ablation craters were 80 μm in diameter. In the recent *Tridacna squamosa*, trace elements were measured next to the grooves from which the stable isotopes were taken, in the same growth increments. In the fossil *Tridacna gigas* shell slice overlapping craters were created along a transect every 16.4 μm resulting in a high-resolution record. The following isotopes

Fig. 1. Map of Indonesia with the location where the *Tridacna gigas* specimen was found.

were measured: ^{24}Mg, ^{26}Mg, ^{27}Al, ^{42}Ca, ^{43}Ca, ^{44}Ca, ^{55}Mn, ^{88}Sr, ^{137}Ba, ^{138}Ba and ^{208}Pb. Trace elemental concentrations were calculated using the natural abundance of calcium, and ratios were calculated with respect to ^{44}Ca. The stable isotope measurements were each assigned a distance on the LA-ICP-MS transect by following the growth lines from which the sample was taken towards the transect line.

To quantify the banding pattern, the gray scale was measured along a line on a photograph of the clam, parallel to the LA-ICP-MS transect, by use of the programme ImageJ (Rasband, 1997), which assigns high values of gray scale to light areas.

3. Results

3.1. Recent Tridacna squamosa

In the *Tridacna squamosa* shell, daily growth increments can be counted in the section of the shell grown in the natural habitat offshore Vietnam (Fig. 2). 365 of these increments span approximately half of this section, suggesting that the specimen grew in its natural habitat for about two years. Towards the hinge of the shell, after the 420th growth increment, lineation becomes too indistinct to be counted. Although no growth increments are visible in the section grown in the aquarium, monitoring of the shell development shows that the growth rate is similar to that in the natural habitat (Fig. 2). In the section grown offshore Vietnam, the δ^{18}O record shows two broad maxima within the inferred one-year period. δ^{18}O varies between −2.24‰ and −1.06‰, with an average of −1.67‰. In the section grown in the aquarium, δ^{18}O values are more negative and less variable (−3.08 to −2.20‰, with an average of −2.52‰). δ^{13}C shows a degree of covariance with δ^{18}O ($R^2 = 0.53$ in the section grown in the natural habitat). However, a strong shift to more negative δ^{13}C values is observed upon the transition from natural to aquarium conditions (Fig. 2).

The minor elemental ratios Mg/Ca, Ba/Ca and Sr/Ca in the *Tridacna squamosa* shell, measured in the same growth increments as δ^{18}O, were not correlated to δ^{18}O and will not be discussed further for this shell. The lack of correlation might be due to the difference in trace element incorporation between different shell zones, as established by Elliot et al. (2009), or to the large amount of scatter in the short period measured. Furthermore, growth rate, calculated from the distance between the daily growth increments, was not correlated to the δ^{18}O, δ^{13}C, Mg/Ca, Ba/Ca or Sr/Ca records (Table 1).

3.2. Miocene Tridacna gigas

In the Miocene *Tridacna gigas* (Fig. 3), δ^{18}O oscillates between −3.0‰ and −1.7‰, with an average of −2.3‰. δ^{13}C varies between 0.5‰ and 2.0‰, with an average of 1.4‰. The average value of δ^{13}C seems to have risen through the lifetime of the clam, while the amplitude of δ^{13}C variability decreased. A comparison of the Mg/Ca and δ^{18}O profiles shows that peaks in the Mg/Ca ratios coincide with low values of δ^{18}O, especially in the later-grown part of the shell. Sr/Ca shows some regularity and a resemblance to the Mg/Ca ratio, but shows no significant correlation with δ^{18}O. In contrast, Ba/Ca shows a negative relation with Mg/Ca, with a slight phase lag. The other trace elemental ratios, Mn/Ca and Pb/Ca, show no clear signal and are not further considered here. Lighter grayscale areas coincide with less negative values of δ^{18}O and low values of Mg/Ca, especially in the latest grown part of the shell (0–2 cm).

4. Discussion

4.1. δ^{18}O as a sea-surface temperature proxy

In previous investigations, the fractionation of stable oxygen isotopes in recent giant clams has been shown to primarily reflect

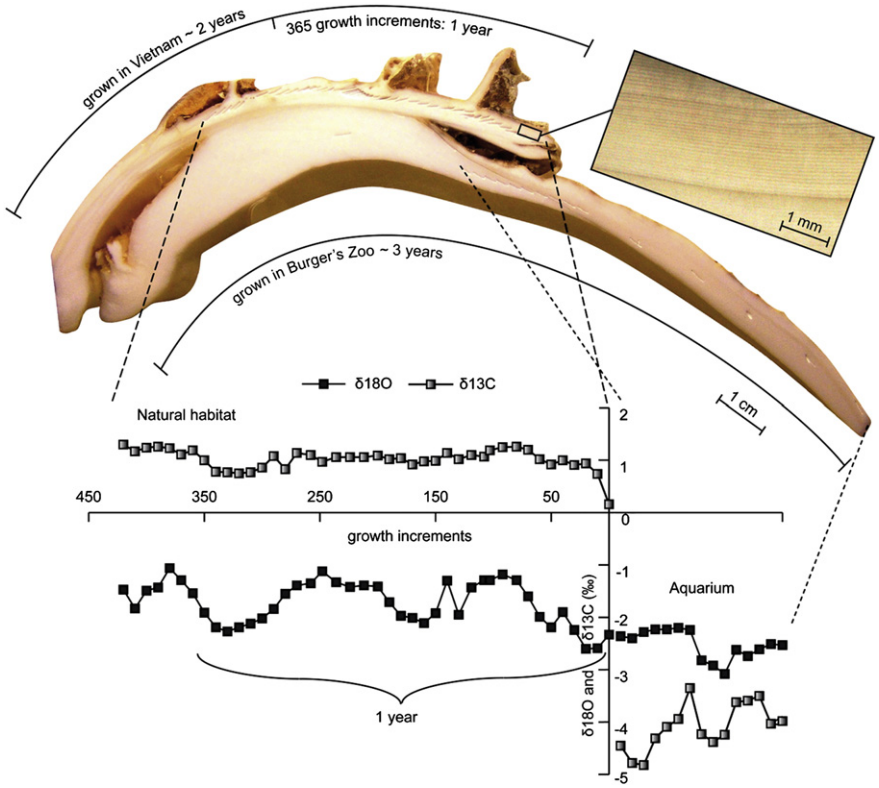

Fig. 2. Slice of the *Tridacna squamosa* shell, with sample grooves and daily growth increments (in adjacent image) with δ^{18}O and δ^{13}C as measured in the part of the shell grown in nature (dashed lines) and in the part of the shell grown in the aquarium (dotted lines).

Table 1
$\delta^{18}O$, $\delta^{13}C$, growth rate, Mg/Ca, Sr/Ca and Ba/Ca as measured in the *Tridacna squamosa* shell.

Tridacna squamosa						
Growth line	$\delta^{18}O$ (‰)	$\delta^{13}C$ (‰)	Growth rate (mm/day)	Mg/Ca mmol/mol	Sr/Ca mmol/mol	Ba/Ca mmol/mol
Shell part grown in nature						
420	−1.47	1.30	0.057			
410	−1.83	1.17	0.057	0.81	1.77	0.0026
400	−1.49	1.24	0.057	1.25	1.91	0.0031
390	−1.43	1.26	0.057	0.80	1.99	0.0044
380	−1.06	1.23	0.055	0.78	1.87	0.0084
370	−1.29	1.11	0.055	0.52	1.74	0.0034
360	−1.54	1.19	0.059	0.53	1.68	0.0029
350	−1.91	1.00	0.062	0.62	1.83	0.0038
340	−2.19	0.78	0.057	0.61	1.74	0.0067
330	−2.27	0.77	0.049	0.66	1.72	0.0050
320	−2.19	0.75	0.047	0.47	1.71	0.0023
310	−2.12	0.77	0.048	0.76	1.84	0.0024
300	−2.02	0.86	0.050	0.55	1.75	0.0035
290	−1.84	1.08	0.049	0.57	1.65	0.0028
280	−1.55	0.83	0.046	1.44	2.04	0.0025
270	−1.39	1.14	0.040	0.85	1.66	0.0054
258	−1.35	1.10	0.037	0.92	1.68	0.0062
248	−1.12	0.97	0.039	0.57	1.50	0.0025
236	−1.33	1.06	0.043	0.50	1.44	0.0016
224	−1.42	1.06	0.044	0.52	1.45	0.0018
212	−1.39	1.06	0.038	0.52	1.45	0.0017
200	−1.41	1.09	0.035	0.60	1.65	0.0024
190	−1.71	1.02	0.038	0.59	1.72	0.0017
180	−1.97	1.04	0.047	0.95	1.93	0.0020
170	−2.01	0.92	0.057	0.82	1.93	0.0020
160	−2.11	0.98	0.061	0.78	1.78	0.0015
150	−1.92	0.99	0.058	0.77	1.89	0.0016
140	−1.30	1.14	0.055	0.94	1.74	0.0017
130	−1.95	1.02	0.052	0.64	1.70	0.0011
119	−1.43	1.10	0.049	0.51	1.72	0.0013
108	−1.29	1.07	0.044	0.46	1.71	0.0028
103	−1.29	1.19	0.044	0.69	2.06	0.0017
92	−1.18	1.25	0.048	1.65	2.84	0.0077
80	−1.29	1.26	0.044	0.78	2.25	0.0032
70	−1.60	1.20	0.046	0.60	2.01	0.0026
60	−1.99	1.02	0.059	1.37	2.08	0.0028
50	−2.19	0.92	0.066	0.73	1.96	0.0016
40	−1.90	1.00	0.063	0.72	1.96	0.0022
30	−2.24	0.91	0.064	0.51	1.73	0.0068
20	−2.60	0.94	0.066	0.55	1.83	0.0023
10	−2.59	0.74	0.066	0.47	1.87	0.0042
0	−2.33	0.16	0.066	0.53	1.89	0.0042
Shell part grown in aquarium						
−10	−2.36	−4.45		0.43	1.81	0.0040
−20	−2.40	−4.78		0.41	1.75	0.0039
−30	−2.28	−4.82		0.42	1.90	0.0046
−40	−2.23	−4.31		0.50	1.87	0.0046
−50	−2.23	−4.09		0.49	2.13	0.0053
−60	−2.20	−3.94		0.50	2.21	0.0057
−70	−2.24	−3.35		0.70	2.13	0.0054
−80	−2.82	−4.23		0.39	2.08	0.0050
−90	−2.92	−4.38		0.37	2.07	0.0049
−100	−3.08	−4.24		0.37	2.01	0.0046
−110	−2.62	−3.62		0.32	1.98	0.0043
−120	−2.74	−3.59		0.35	1.86	0.0042
−130	−2.61	−3.50				
−140	−2.51	−4.03				
−150	−2.53	−3.98				

temperature and hydrologic variations (Aharon, 1991; Lin et al., 2006; Elliot et al., 2009). The $\delta^{18}O$ from tridacnid species has been applied to reconstruct ice volume variations over the last 100 kyr (Aharon, 1983; Aharon and Chappell, 1986), to reconstruct decadal climate variability in the Holocene (Watanabe et al., 2004), and the ENSO system in the Holocene and Pleistocene (Welsh et al., 2005; Ayling et al., 2006; Elliot et al., 2006). In addition, trace elemental ratios such as Mg/Ca and Ba/Ca have been compared to $\delta^{18}O$ and were shown to reflect seasonal variations in climatic parameters (Elliot et al., 2003; Ayling et al., 2006; Elliot et al., 2009).

The $\delta^{18}O$ record of our Vietnamese *Tridacna squamosa* may be used to establish the sensitivity of *Tridacna* to environmental variability, since the life of this specimen has been divided between a highly-seasonal natural environment and the controlled conditions of an aquarium. The $\delta^{18}O$ record of the shell section grown in the natural environment follows a pattern of two minima within a one-year period (Fig. 2). This semi-annual pattern in $\delta^{18}O$ is in agreement with the annual sea surface temperature development along the coast of Vietnam, where the *T. squamosa* specimen originates. In June, the southwest monsoon causes upwelling on the coast of South Vietnam, while in July and August, the cold upwelled water spreads northeastward, causing a basin-wide mid-summer cooling in the South China Sea (Xie et al., 2003). Hence, $\delta^{18}O$ in *Tridacna* appears to faithfully record sea-surface temperature variability with seasonal resolution.

Assuming temperature to exert the dominant control over $\delta^{18}O$ in giant clam shells, the following formulas were developed by Aharon (1983) (Eq. (1)) and Grossman and Ku (1986) (Eq. (2)), in which $\delta^{18}O_{aragonite}$ represents shell carbonate and δ_w represents $\delta^{18}O$ of sea water:

$$T(^{\circ}C) = 21.3 - 4.42^{*}\left(\delta^{18}O_{aragonite} - \delta_w\right) \quad (1)$$

$$T(^{\circ}C) = 21.8 - 4.69^{*}\left(\delta^{18}O_{aragonite} - \delta_w\right) \quad (2)$$

To test the robustness of these relationships for the present study, the formulas were applied to the $\delta^{18}O$ values measured in the section of the *Tridacna squamosa* grown in the aquarium, where all required variables were well-constrained. δ_w of the aquarium water was −1.05‰, and the average $\delta^{18}O$ of the first seven shell measurements, all taken at a constant distance from the shell edge, was −2.3‰ (Fig. 2). This generates temperatures of 26.8 °C and 27.7 °C via the two formulas, respectively, thus within 1–2 °C of the true temperature of the aquarium (Fig. 4). Assuming the $\delta^{18}O_{aragonite}$ vs. temperature relationship for both *Tridacna* specimens to run parallel to those of Aharon (1983) and Grossman and Ku (1986), the range of $(\delta^{18}O_{aragonite} - \delta_w)$ values for the section of the *T. squamosa* shell grown in the natural environment (assumed $\delta_w = -0.28$‰), and the Miocene *Tridacna gigas* (assumed $\delta_w = -0.88$), suggest that both shells experienced ambient temperature fluctuations up to 5–7 °C. However, these ranges must be regarded as maximum estimates, since the potential influence of salinity on $\delta^{18}O_{aragonite}$ (i.e. via seasonal changes in ambient δ_w) is not included in the calculation.

4.2. $\delta^{18}O$, elemental and visual records in the Miocene *Tridacna gigas*

The $\delta^{18}O_{aragonite}$ record of the Miocene *Tridacna gigas* shell displays pronounced oscillations (Fig. 3). On the basis of the coupling between sea surface temperature variability offshore Vietnam and $\delta^{18}O_{aragonite}$ in the modern *Tridacna squamosa*, we interpret the oscillations in $\delta^{18}O_{aragonite}$ of the Miocene *T. gigas* primarily as a SST record. However, since there is no specific evidence for a semi-annual upwelling cycle in the paleolocation of the *T. gigas* specimen, we tune the peaks in the $\delta^{18}O_{aragonite}$ record to one cycle per year (Fig. 3), in accordance with the modern annual SST cycle around west Java and the approach of Elliot et al. (2009). The range of $\delta^{18}O$ values does not show a trend corresponding with the clams' ontogeny, confirming that the influence of growth stage on $\delta^{18}O$ was minimal. Furthermore, diagenetic alteration of the *T. gigas* specimen is unlikely, as a banding pattern is clearly discernible and no large crystals were observed in the biomineralogical matrix. Also, the $\delta^{18}O$ record shows no trend from the core to the rim of the shell, and the clear and well-defined pattern in $\delta^{18}O$ and in the trace-elemental ratios has a large amplitude, which may be erased by on-going diagenesis.

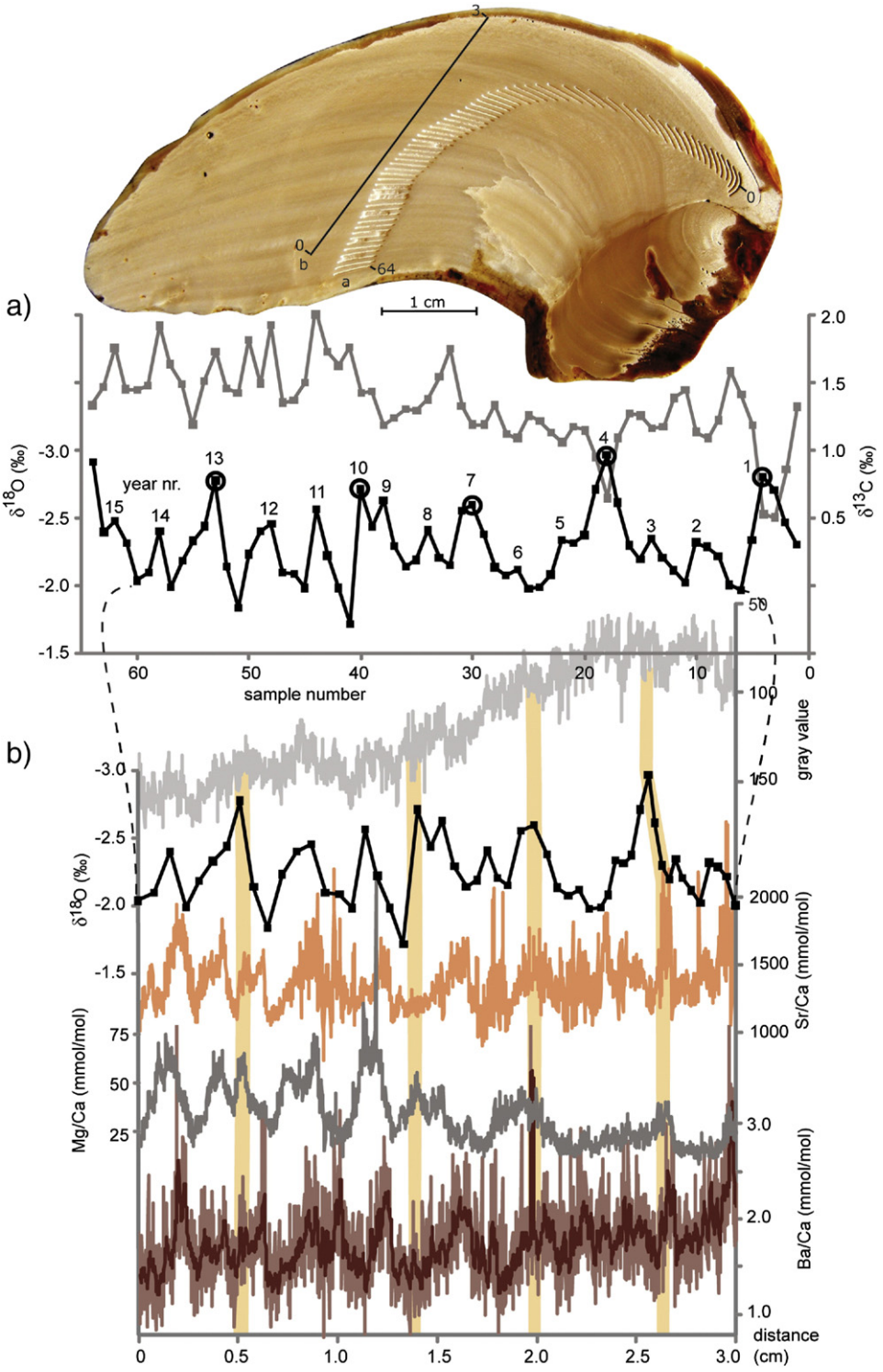

Fig. 3. Slice of the *Tridacna gigas* shell, with sample grooves (a) and laser ablation transect (b). a) $\delta^{18}O$ and $\delta^{13}C$ as measured from each sample groove, with circles indicating the shifts to negative values; b) Mg/Ca, Sr/Ca and Ba/Ca (with a 9-point moving average) as measured along the laser ablation transect, compared to $\delta^{18}O$ with an assigned distance on this transect, and gray value measured parallel to this line.

The negative correlation of Mg/Ca and $\delta^{18}O$ in *Tridacna gigas* suggests that shell Mg/Ca also responds to the annual SST cycle. However, the correlation is more robust in the later grown section of the shell (between the 6th and 14th measured year), than in the earlier-grown section, as observed in a previous study (Elliot et al., 2009). Hence, our data confirms the qualitative use of *Tridacna* shell Mg/Ca as a SST proxy, but also the quantitative limitations with respect to $\delta^{18}O$. Similarly, the darkness of the shell's annual growth bands (Bonham, 1965; Aharon, 1991) can be more easily correlated to $\delta^{18}O$ with increasing age. Specifically, dark bands coincide with lower values of $\delta^{18}O$ (and thus higher values of Mg/Ca), suggesting these were formed during the warmer season. Micromill sampling started at a slight distance from the shell edge, implying that the first 1 or 2 years of the lifespan of the *T. gigas* have not been included in our

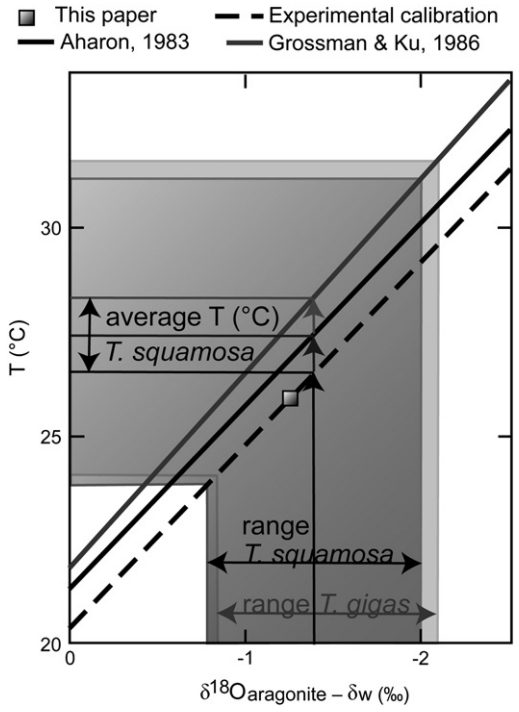

Fig. 4. Temperature against $\delta^{18}O_{aragonite}$–$\delta^{18}O_{water}$, with the formula of Aharon (1983), the formula of Grossman and Ku (1986), the data point from the shell part grown in the aquarium and the values of the recent *Tridacna squamosa* and the Miocene *Tridacna gigas* (black lines represent the average values).

analyses. This suggests that the increase in strength of correlation between the various proxies is located between 7 and 8 years of age in this specimen.

Ba/Ca in the *Tridacna gigas* appears to be negatively correlated to Mg/Ca, but with a slight phase lag between Mg/Ca troughs and Ba/Ca peaks. A similar relationship between shell Mg/Ca and Ba/Ca was observed by Elliot et al. (2009). Furthermore, Ba/Ca was shown by these authors to display a consistent signal throughout the *Tridacna* shell, indicating robust, growth-independent incorporation and thus a strong potential for environmental reconstruction. However, the precise environmental information stored in shell Ba/Ca remains debated. Although river discharge may alter ambient seawater Ba/Ca, and consequently the background shell Ba/Ca of mollusks (Gillikin et al., 2006), the required magnitude of Ba-rich freshwater pulses would be too great for these to explain the Ba/Ca peaks observed in *Tridacna* shells (Elliot et al., 2009). Ingestion of phytoplankton, which may contain over 400 nmol/g barite (Dehairs et al., 1980), has been suggested as a means of focusing Ba within mollusks, although this mechanism also appears to require a seasonal cycle of the barium partition coefficient into shell aragonite to explain the range of Ba/Ca peaks in *Tridacna* shells (Elliot et al., 2009). Nevertheless, Elliot et al. (2009) observed a correlation between the timing of chlorophyll maxima and shell Ba/Ca maxima in several Pacific *Tridacna* shells, suggesting that primary productivity ultimately controls the timing of the Ba/Ca fluctuations observed in our *T. gigas* specimen.

4.3. Interannual variability and Miocene ENSO

An apparent pattern is observed in the $\delta^{18}O$ record of the *Tridacna gigas*, in which every third annual negative excursion is more extreme than the preceding two (circles in Fig. 3). Time series analyses were performed on this series with the program Redfit (Schulz and Mudelsee, 2002), which estimates red-noise spectra for unevenly spaced data series. This confirms dominant periodicities of 1 and 2.9 years in the $\delta^{18}O$ record (Fig. 5). Mg/Ca shows similar dominant periodicities of 1.0 and 3.0 years (Fig. 5). Due to the short nature of the records, the significance of the peaks is relatively low, as indicated by the χ^2 significance levels (Fig. 5). Nevertheless, the $\delta^{18}O$ record in particular shows a robust and regular interannual oscillation within the lifespan of the *Tridacna gigas*.

The tri-annual negative shifts in the $\delta^{18}O$ and Mg/Ca records indicate regular deviations to warmer conditions in the Miocene West Pacific, resembling the signal of present-day La Niña events (Aldrian and Susanto, 2003). This evidence for strong interannual SST variability in the West Pacific during the Miocene supports the interpretation of ENSO-like variability recorded in a late-Miocene laminite record from modern-day Italy (Galeotti et al., 2010). ENSO variability has been proposed to be reduced during warmer intervals of Cenozoic climate history, as recently as the Pliocene (Ravelo et al., 2006), due to a globally deeper thermocline and thus a reduced temperature gradient in the Pacific. Furthermore, the paleoceanography of the Pacific has not always been conducive to sustaining east–west oscillations of surface water masses. Most notably, the Panamanian gateway remained open until the early Pliocene (Haug and Tiedemann, 1998) and restriction of deep water throughflow across Indonesia probably began only in the Oligocene (Kuhnt et al., 2004). Yet, fully coupled ocean–atmosphere modeling experiments of the Miocene still show robust ENSO variability (Galeotti et al., 2010). Our new evidence supports the inference that such interannual variability persisted during the Miocene, despite the apparently less favorable tectonics and heat distribution of this epoch. Climate cooling during the Middle Miocene climate transition (~ 14 Ma years ago) and a progressively more modern tectonic configuration may have provided appropriate boundary conditions to create “near-modern” oceanic conditions in the Indo-Pacific (Flower and Kennet, 1994; Tian et al., 2009). According to Leckie and Nathan (2007), formation of a proto-warm pool took place in the intervals of 11.6 to 9.6 Ma and from 6.5 to 6.1 Ma. Our Tridacnid clam, with an age of 10 to 13 Ma, thus potentially records the development of ENSO during the first restriction of the Indonesian throughflow starting at 11.6 Ma. However, it has been suggested that earlier, even warmer climatic

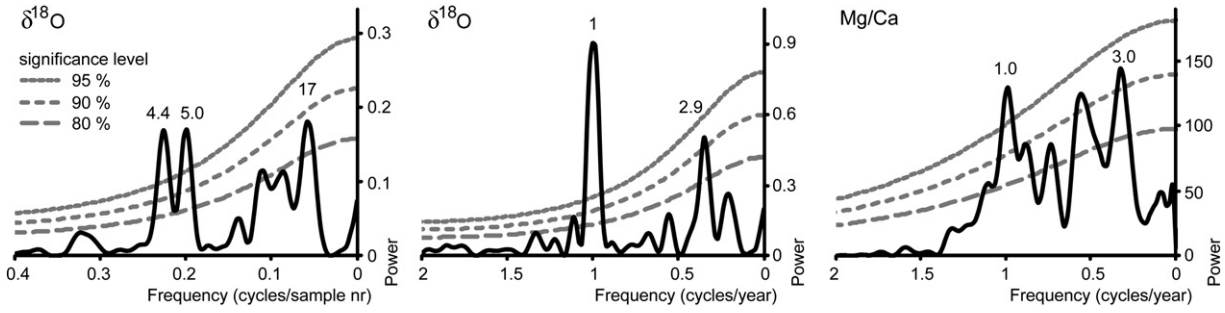

Fig. 5. Spectral analysis by Redfit of $\delta^{18}O$ and Mg/Ca from *T. gigas* with major periodicities and χ^2 significance levels indicated. From left to right: – $\delta^{18}O$ in the spatial domain (sample number); – $\delta^{18}O$ in the time domain (years); – Mg/Ca in the time domain (years).

intervals such as the Eocene, also experienced ENSO-type climate variability (Huber and Caballero, 2003). New seasonally-resolved climate records from such intervals are still required to corroborate this theory.

5. Summary

Shell carbonate $\delta^{18}O$ of a modern *Tridacna squamosa* giant clam has been shown to record the annual sea-surface temperature (SST) pattern of its natural environment, and the stable temperatures of a controlled aquarium environment after transplantation. Using this evidence and established relationships between $\delta^{18}O$ and SST, oscillations in $\delta^{18}O$ with age in a Miocene *Tridacna gigas* specimen have been tuned to represent yearly SST variability during the growth of the shell. $\delta^{18}O$ in the *T. gigas* is anti-correlated to (and in-phase with) Mg/Ca, suggesting that Mg/Ca is also controlled by temperature. Ba/Ca is negatively correlated to Mg/Ca, but shows a phase lag of several months, suggesting that the primary productivity cycle controlling shell Ba/Ca was offset from the annual SST cycle. Tri-annual shifts to more negative values of $\delta^{18}O$ and Mg/Ca may reflect the occurrence of La Niña-like events within a pattern of interannual climate variability resembling ENSO. The inferred presence of such variability during the Miocene epoch challenges current theories of permanent El Niño-like conditions during warmer climatic intervals.

Acknowledgements

We would like to thank Arnold van Dijk, Gijs Nobbe, Otto Stiekema and Helen de Waard for their technical support. Also, we would like to thank Simone Galeotti and an anonymous reviewer, as well as the editor, Thierry Corrège, for their useful comments.

References

Aharon, P., 1983. 140,000-yr isotope climatic record from raised coral reefs in New Guinea. Nature 304, 720–723.
Aharon, P., 1991. Recorders of reef environmental histories: stable isotopes in corals, giant clams, and calcareous algae. Coral Reefs 10, 71–90.
Aharon, P., Chappell, J., 1986. Oxygen isotopes, sea level changes and temperature history of a coral reef environment in New Guinea over the last 105 years. Palaeogeography, Palaeoclimatology, Palaeoecology 56, 337–379.
Aldrian, E., Susanto, R.D., 2003. Identification of three dominant rainfall regions within Indonesia and their relationship to sea surface temperature. International Journal of Climatology 23, 1435–1452.
Ayling, B.F., Chappell, J., McCulloch, M.T., Gagan, M.K., Elliot, M., 2006. High-resolution paleoclimate of the MIS 11 interglacial (423–360 ka) using geochemical proxies in giant Tridacna clams. Geochimica et Cosmochimica Acta 70 (18), A26.
Bonham, K., 1965. Growth rate of giant clam Tridacna gigas at Bikini Atoll as revealed by radioautography. Science 149, 300–302.
Cane, M.A., 2005. The evolution of El Niño, past and future. Earth and Planetary Science Letters 230, 227–240.
Chaisson, W., 1995. Planktonic foraminiferal assemblages and paleoceanographic change in the trans-tropical Pacific Ocean; a comparison of west (Leg 130) and east (Leg 138), latest Miocene to Pleistocene. Proceedings of the Ocean Drilling Program, Scientific Results 138, 555–597.
Dehairs, F.A., Chesselet, R., Jedwab, J., 1980. Discrete suspended particles of barite and the barium cycle in the open ocean. Earth and Planetary Science Letters 49, 40–42.
Elliot, M., Gagan, M., McCulloch, M., Cabioch, G., 2003. Trace element and stable isotope profiles of modern giant-long-lived Tridacna maxima from New Caledonia: potential applications to paleo-environmental studies. EGS-AGU-EUG Joint Assembly, Geophysical Research Abstracts, vol. 5, p. 12904.
Elliot, M., Welsh, K., Yokoyama, Y., McCulloch, M., Chappell, J., 2006. Holocene records of Western Pacific Warm Pool paleoclimate using fossil long-lived giant Tridacna from Papua New Guinea. Eos Transactions American Geophysical Union 87 (52) Fall Meeting Supplement, PP43A-1209.
Elliot, M., Welsch, K., Chilcott, C., McCulloch, M., Chappell, J., Ayling, B., 2009. Profiles of trace elements and stable isotopes derived from giant long-lived *Tridacna gigas* bivalves: potential applications in paleoclimate studies. Palaeogeography, Palaeoclimatology, Palaeoecology 280, 132–142.
Fedorov, A.V., Dekens, P.S., McCarthy, M., Ravelo, A.C., deMenocal, P.B., Barreiro, M., Pacanowski, R.C., Philander, S.G., 2006. The Pliocene Paradox (mechanisms for a permanent El Niño). Science 312, 1485–1489.
Flower, B.P., Kennet, 1994. The middle Miocene climatic transition: East Antarctic ice sheet development, deep ocean circulation and global carbon cycling. Palaeogeography, palaeoclimatology, palaeoecology 108 (3–4), 537–555.
Galeotti, S., von der Heydt, A., Huber, M., Bice, D., Dijkstra, H., Jilbert, T., Lanci, L., Reichart, G.J., 2010. Evidence for active ENSO variability in the late Miocene greenhouse climate. Geology 38 (5), 419–422.
Gerth, H., 1921. Coelenterata. Sammlungen des Geologischen Reichs-Museums in Leiden. Neue Folge 1 (2), 387–445.
Gillikin, D.P., Dehairs, F., Lorrain, A., Steenmans, D., Baeyens, W., André, L., 2006. Barium uptake into the shells of the common mussel (*Mytilus edulis*) and the potential for estuarine paleo-chemistry reconstruction. Geochimica et Cosmochimica Acta 70, 395–407.
Grossman, E.L., Ku, T.-L., 1986. Oxygen and carbon isotope fractionation in biogenic aragonite: temperature effects. Chemical Geology 59, 59–74.
Haug, G.H., Tiedemann, R., 1998. Effect of the formation of the Isthmus of Panama on Atlantic Ocean thermohaline circulation. Nature 393, 673–676.
Huber, M., Caballero, R., 2003. Eocene El Niño: evidence for robust tropical dynamics in the "Hothouse". Science 299, 877–881.
Kuhnt, W., Holbourn, A., Hall, R., Zuvela, M., Käse, R., 2004. Neogene history of the Indonesian Throughflow. In: Continent–ocean interactions within East Asian Marginal Seas. Geophysical Monograph Series 149, 299–320.
Leckie, R., Nathan, S.A., 2007. Closure of the Indonesian Seaway during the middle to late Miocene (13.2–5.8 Ma). Early history of the Western Pacific Warm Pool. Eos Transactions American Geophysical Union 88 (52) Fall Meeting Supplement, PP11A-0200.
Lin, Y., Mii, H., Li, K., 2006. Oxygen isotope evidence for higher summer temperature in Tridacna maxima shells from Southern Taiwan, 4,000 B.P. Eos Transactions American Geophysical Union 88 (52) Fall Meeting Supplement, PP43A-1211.
Martin, K., 1911. Vorläufiger Bericht über geologische Forschungen aauf Java. Erster teil. Sammlungen des Geologischen Reichs-Museums in Leiden 1e serie, vol. 9, pp. 1–76.
Martin, K., 1919. Unsere Paläozoologische Kenntnis von Java. E.J. Brill, Leiden. 158 pp.
Martin, K., 1921. Molluska. Sammlungen des Geologischen Reichs-Museums in Leiden. Neue Folge 1 (2) 387-446-470.
McConnaughey, T., 1989. ^{13}C and ^{18}O isotopic disequilibrium in biological carbonates: II. In Vitro simulation of kinetic isotope effects. Geochimica et Cosmochimica Acta 53, 163–171.
McGregor, H.V., Gagan, M.K., 2003. Diagenesis and geochemistry of Porites corals from Papua New Guinea: implications for paleoclimate reconstruction. Geochimica et Cosmochimica Acta 67, 2147–2156.
Meyers, G., 1996. Variation of Indonesian throughflow and the El Niño-Southern Oscillation. Journal of Geophysical Research 101 (C5), 12255–12263.
Rasband, W.S., 1997–2007. Image J. U. S. National Institutes of Health, Bethesda, Maryland, USA. http://rsb.info.nih.gov/ij/.
Ravelo, A.C., Dekens, P.S., McCarthy, M., 2006. Evidence for El Niño-like conditions during the Pliocene. GSA Today 16, 4–11.
Rickaby, R.E.M., Halloran, P., 2005. Cool La Niña During the Warmth of the Pliocene? Science 307, 1948–1952.
Schulz, M., Mudelsee, M., 2002. REDFIT: estimating red-noise spectra directly from unevenly spaced paleoclimatic time series. Computers & Geosciences 28, 421–426.
Tian, J., Shevenell, A., Wang, P., Zhao, Q., Li, Q., Cheng, X., 2009. Reorganization of Pacific Deep Waters linked to middle Miocene Antarctic cryosphere expansion: a perspective from the South China Sea. Palaeogeography, Palaeoclimatology, Palaeoecology 284 (3–4), 375–382.
van der Vlerk, I.M., 1921. Foraminiferen uit het Tertiair van Java 1. Wetenschappelijk Mededeelingen dienst mijnbouw in Bandoeng, vol. 1, pp. 16–35.
Wang, C. And, Fiedler, P.C., 2006. ENSO variability and the eastern tropical Pacific: a review. Progress in Oceanography 69, 239–266.
Wara, M.W., Ravelo, A.C., Delaney, M.L., 2005. Permanent El Niño-like conditions during the Pliocene warm period. Science 309, 758–761.
Watanabe, T., Suzukib, A., Kawahata, H., Kan, H., Ogawa, S., 2004. A 60-year isotopic record from a mid-Holocene fossil giant clam (*Tridacna gigas*) in the Ryukyu Islands: physiological and paleoclimatic implications. Palaeogeography, Palaeoclimatology, Palaeoecology 212, 343–354.
Welsh, K.J., Elliot, M., Chappel, J., 2005. Probing the climate of the Western Pacific Warm Pool during a perturbed thermohaline circulation (10–60 Ka) using oxygen isotopes from long lived fossil bivalves. Eos Transactions American Geophysical Union 86 (52) Fall Meeting Supplement, PP12B-02.
Xie, S.-P., Xie, Q., Wang, D., Liu, W.T., 2003. Summer upwelling in the South China Sea and its role in regional climate variations. Journal of Geophysical Research 108 (C8), 3261.